

Non-Hermitian exciton dynamics in a photosynthetic unit system

A. Thilagam*

*Information Technology, Engineering and Environment,
Mawson Institute, University of South Australia, Australia 5095*

The non-Hermitian quantum dynamics of excitonic energy transfer in photosynthetic systems is investigated using a dissipative two-level dimer model. The approach is based on the Green's function formalism which permits consideration of decoherence and intersite transfer processes on comparable terms. The results indicate a combination of coherent and incoherent behavior at higher temperatures with the possibility of exceptional points occurring at the coherent-incoherent crossover regime at critical temperatures. When each dimer site is coupled *equally* to the environmental sources of dissipation, the excitonic wavepacket evolves with time with a coherent component, which can be attributed to the indistinguishability of the sources of dissipation. The time evolution characteristics of the B850 Bchls dimer system is analysed using typical parameter estimates in photosynthetic systems, and the quantum brachistochrone passage times are obtained for a range of parameters.

PACS-number(s): 71.35.-y, 03.65.Yz, 03.67.Mn

I. INTRODUCTION

The theory of excitonic energy transfer has been a topic of interest over several decades in light harvesting systems (LHS) [1–15]. The Fenna–Matthews–Olson (FMO) complex of the green sulfur bacteria [16–19] constitutes the prototypical LHS for modelling photosynthetic activities [9, 20, 21], mainly due to its generic features of energy transfer also seen in other photosynthetic systems [5–7]. In the FMO complex, two types of light-harvesting molecular systems complexes, known as LH1 and LH2, perform different roles. The LH1 is directly linked with the reaction center (RC) unlike the LH2 complex which interacts with the RC via LH1. The main attraction in light harvesting systems is the exceptionally high efficiencies at which excitation propagates between the light harvesting complexes before reaching the reaction center (RC) pigment protein complex [3, 6, 7]. In fact, the quantum efficiency in transfer at low illumination intensities reaches close to a value of unity. The importance of mimicking the transfer processes seen in LHS has obvious applications in artificial light harvesting system such as Ruthenium based complexes [22–24]. To this end, accurate knowledge of the underlying mechanisms of energy transport and the process by which excess energy in excited states is transferred to their surroundings in LHS is critical to the development of potential sources of energy generation [25–28].

Early experimental work in 1960 by Chance and Nishimura [4] showed that some level of photosynthetic activity occurred in chlorophyll systems close to room temperatures (300 K). The occurrence of quantum coherence during photosynthesis was not obvious due to the level of precision of the apparatus employed at that time. However recent progress in experimental techniques such as two-dimensional Fourier transform electronic spectroscopy (2DFTES) [16, 18, 29, 30] has confirmed that quantum coherence is indeed conserved for relatively long times (up to 1 picosecond) in excited states. Using 2DFTES [18], the FMO complex of green sulfur bacteria showed a surprisingly long coherence time of about 700 fs at 77 K, and also at room temperatures (277 K) in a related work [31]. These ambient temperatures are generally considered adverse for quantum features such as superpositions and non-classical correlations to be maintained for a reasonable period of time. However the experimental results [16, 18, 29–31] appear to suggest the critical role played by non-local quantum effects in energy transfer mechanisms in LHS. To this end, the application of advanced measurement tools involving spectrally resolved, 4-wave mixing measurements [32] is expected to introduce greater depth to the study of quantum correlations in photosynthetic systems which undergo both decoherence and dissipation due to interactions with the environment.

Galve et. al. [33] showed recently that for a system of two interacting and parametrically driven harmonic oscillators undergoing dissipation, entanglement can exist at any temperatures. Although this specific quantum system appear distinct from quantum models which describe LHS, the general consensus is that the slower processing speed inherent in classical models is inadequate for LHS compared to the processing attributes of quantum systems. This viewpoint has been the focus of many recent works [9, 34–40] involving LHS. A variety of methods involving the Red-field approach employing the Born-Markov and secular approximations [41–43], the non-Markovian approach which involves solving the integrodifferential equation using perturbation theory [44], and recently the more sophisticated

*Electronic address: thilaphys@gmail.com

and numerically intensive reduced hierarchy equation approach [45] have been employed to examine the propagation of excitation in LHS. In light-harvesting complexes with strong system-bath coupling, a generalized BlochRedfield (GBR) equation approach was used to show that optimal efficiency in energy transfer cannot be optimized with respect to the temperature and spatialtemporal correlations in noise [46]. Thus classical approaches to the excitonic transport which involve the hopping model [1, 2, 5] have given way to more sophisticated quantum mechanical models of exciton propagation [9, 11, 45–47] which incorporate quantum coherence aspects during the energy transfer process.

Greens functions are known to provide an effective description of the quantum evolution of non equilibrium quantum processes [49–53], and here we use this approach to examine the influence of dissipative processes on the dynamical evolution of the exciton population in LHS. While several works have considered coherence and bath correlations [34, 35, 48] as possible factors for the high efficiencies of LHS, here we consider two features which may account for the quantum properties in LHS: (a) the persistence of coherence when the dissipative coupling of each monomer to its surrounding environment becomes equivalent to that of the adjacent monomer, and (b) the appearance of exceptional points at critical temperatures. The simple model of the dimer is used to show that in the event that the coupling of each subsystem to the phonon bath or other sources of dissipation is equal, the overall time evolution still retains a coherent component, an idea that was first proposed by Stafford and Barrett [65] in the context of the decay of super deformed nuclei systems. This key feature implies that a degree of coherence is maintained even at temperatures that would otherwise be considered adverse for any superpositions of the quantum states. Accordingly we consider the maintenance of coherence, as quantified by the time duration of oscillations in the population difference at the two site model, as a measure of the photosynthetic efficiency. In general, the photon is absorbed by a network system of pigments and transported to the reaction center (RC) trap so that efficiency is based on the success of being trapped at the RC. The connection between quantum coherence and photosynthetic efficiency is justified as the loss of coherence disrupts the likelihood of the propagating exciton of reaching its destination due to decoherence processes.

Unlike earlier works on LHS, we take advantage of the non-Hermitian features inherent in any open quantum system which encounter dissipative forces. We also aim to examine the underlying factors which are linked with the non-Hermitian features and which may account for the observed long-lived coherence in LHS. Open quantum systems with non-Hermitian components evolve in ways which are vastly different from quantum systems associated with a purely Hermitian Hamiltonian. For instance, the states associated with an Hermitian Hamiltonian have long lifetimes, while those of the non-Hermitian Hamiltonian have a finite lifetime. Non-Hermitian resonances are associated with complex eigenvalues with real (imaginary) component that yield the energy (resonance width), and possess non-orthogonal eigenvectors. Thus states which are orthogonal under the ordinary inner product in the Hermitian quantum space are allowed to be non-orthogonal in the non-Hermitian case. The real state energies of a Hermitian Hamiltonian give rise to the avoided level crossing [54] when a single parameter is varied, which is not necessarily true in the case of a non-Hermitian Hamiltonian. The presence of non-Hermitian terms is critical to the occurrence of dynamical phase transitions as well. Moreover the appearance of degeneracies such as exceptional points (EPs) is a unique feature of non-Hermitian quantum systems, and may assist in distinguishing classical and quantum modes of transport in LHS.

A topological defect like the exceptional point occurs when two eigenvalues of an operator coalesce as a result of change in selected system parameters, and the two mutually orthogonal states merge into one self-orthogonal state, resulting in a singularity in the spectrum [55]. The critical parameter values at which the singularity appear are called exceptional points. A notable feature associated with exceptional points is the violation of the adiabatic theorem, that is the switching of an initial eigenstate to another eigenstate when the system parameters are altered adiabatically around the exceptional point. In contrast, Hermitian systems exhibit only berry phases [56], with no change in the initial eigenstate as the system parameters are altered adiabatically. Thus no exceptional points can exist in Hermitian systems and at degenerate points the eigenstates exist only in a two-dimensional subspace spanned by vectors. EPs have been observed in experiments involving microwave billiards [57–59], semiconductors cavities [60] and photo-dissociated vibronic resonance states of the H_2^+ molecular ion [61]. Exceptional points may be associated with the transition or crossover points at which coherent to incoherent tunnelling occur in open quantum systems. The detection of the exceptional points are still under active investigation [62]. One possible technique involves the detection of the switching process, in which two states around an exceptional point swap states and thus behave distinctly from other states which remain unchanged when the selected parameter is changed adiabatically [63]. However the experimental detection of such topological changes still remains a challenge.

This work is organized as follows: In Sec. (II) we present the theory of the exciton transfer using Green’s function formalism and analyse the influence of the intersite coupling energy and dissipation rates on the coherence properties of the exciton in a simple dimer system. In Sec. (III), we examine the photosynthetic qubit system and discuss the conditions under which exceptional points appear. In Sec. (IV), the dimer model is applied to the B850 Behls system and numerical estimates of the time scales of coherent oscillations in the exciton population difference are obtained. Estimates of the critical temperatures at which exceptional points occur are also evaluated for a range of environmental dissipation strength differences. Lastly, in Sec. (V), the quantum brachistochrone passage times are obtained for a range of parameters in photosynthetic systems. A brief discussion and conclusion are also provided in

Sec. (V).

II. EXCITON TRANSFER USING GREEN'S FUNCTION FORMALISM

The Hamiltonian describing the propagation of the exciton in molecular systems is based on the tight-binding model [52]

$$\hat{H}_{ex} = \sum_l \left[\Delta E + \sum_{m \neq l} D_{l,m} \right] B_l^\dagger B_l + \sum_{m \neq l} V B_l^\dagger B_m \quad (1)$$

where B_j^\dagger (B_j) is the creator (annihilation) exciton operator at site j . ΔE , the on-site excitation energy and $D_{l,m}$ is the dispersive interaction matrix element which determines the energy difference between a pair of excited electron and hole at a molecular site and ground state electrons at neighboring sites [52]. V the exciton transfer matrix element between molecular sites at l and m . In the case of the dimer system with just two coupled sites (labeled l and m), Eq. (1) is greatly simplified

$$\hat{H}_{ex} = E_l^0 B_l^\dagger B_l + E_m^0 B_m^\dagger B_m + V B_l^\dagger B_m \quad (2)$$

where E_l, E_m are the exciton energies at sites l, m and the subscript 0 denotes the absence of lattice site fluctuations.

In the presence of a non-Hermitian decay terms and phonon bath reservoirs at each site, the exciton dynamics of the dimer system is determined by the following Hamiltonian

$$\hat{H}_T = \hat{H}_{ex} + \hat{H}_d + \hat{H}_p + \hat{H}_{ep} \quad (3)$$

$$\hat{H}_d = i \sum_{j=l,m} \zeta_j B_j^\dagger B_j \quad (4)$$

$$\hat{H}_p = \sum_{j=l,m} \sum_q \hbar \omega(q, j) b_{q,j}^\dagger b_{q,j} \quad (5)$$

$$\hat{H}_{ep} = N^{-1/2} \sum_{j=l,m} \sum_q F_j(q) B_j^\dagger B_j (b_{-q,j}^\dagger + b_{q,j}) \quad (6)$$

where the isolated exciton Hamiltonian, \hat{H}_{ex} is given in Eq. (2). We allow the intersite tunnelling amplitude V to be influenced by a phonon correlated environment via a Franck-Cordon (FC) factor [64]

$$V_r = V \exp \left[- \int_0^\infty \frac{J(\omega)}{\omega^2} \coth \left(\frac{\hbar \omega}{2k_B T} \right) d\omega \right] \quad (7)$$

where the spectral density function is given by $J(\omega) = \sum_q |F_a(q)|^2 \delta(\omega - \omega_q)$. We assume that the correlated exciton-phonon interaction term $F_a(q)$ to be the average ($\frac{1}{2}[F_l(q) + F_m(q)]$) of the interactions at sites, l, m . The argument of the exponential term in Eq. (7) is known as the FC factor [64] and its dependency on the temperature varies according to the form chosen for $J(\omega)$.

The non-Hermitian dissipative Hamiltonian in Eq. (4), \hat{H}_d is associated with ζ_j , the decay rate of the exciton at each site $j = l, m$. For simplicity in numerical analysis, we have incorporated several processes such as exciton annihilation due to recombination and trapping effects into ζ_j , with the requirement that the decay rate is dependent on the site j . Due to differences in environmental conditions at the two sites of the dimer $\zeta_l \neq \zeta_m$, however the possibility that $\zeta_l \approx \zeta_m$ cannot be excluded. \hat{H}_p denotes the sum of phonon energies at the two sites and $b_{q,j}^\dagger$ ($b_{q,j}$) is the creation (annihilation) phonon operator associated with the phonon bath at site j , with frequency $\omega(q)$ and wavevector q . \hat{H}_{ep} represents the sum of the exciton-phonon interactions at the two sites, and $F_j(q)$ quantifies the interaction strength which is assumed to be linear in the phonon operators and which is dependent only on the phonon wavevector q . We consider that both dissipation and dephasing processes occur as a consequence of exciton-phonon interactions. The dissipative mechanisms associated with the exciton-phonon interactions introduce a non-Hermitian term in the Green's function (see Eq. (10) below) which account for the irreversible loss in the exciton population. While the dephasing term leaves the overall exciton population unchanged, it contributes to incoherence by changing the non-diagonal components of the density matrix.

The Green's function for an exciton at time t which yields the dynamical measure of the amplitude of the electron (hole) to propagate forward (backward) in time is given by [52]

$$G_{l,m}(t) = -i\Theta(t)\langle \{B_l(t)B_m^\dagger\} \rangle \quad (8)$$

where $\Theta(t)$ denotes the step function and the exciton Green's function is averaged over the quantum mechanical properties of the propagating excitonic wavefunction that is dependent on the phonon bath and contribution from the dissipative terms. Following the approach by Stafford and Barrett [65], the Fourier transform $G_{l,m}(E)$ is given in terms of the energy E as $G_{l,m}(E) = \int_{-\infty}^{\infty} dt G_{l,m}(t) e^{iEt}$. For the simple case of the dimer system with two coupled sites of energies E_l, E_m , the inverse of the Green's function $G_{l,m}(E)$ is obtained as

$$G_{l,m}^{-1}(E) = \begin{bmatrix} E - E_l - \Delta_l + i\eta + & -V_r \\ -V_r & E - E_m - \Delta_m + i\eta + \end{bmatrix} - \frac{1}{2}\Sigma. \quad (9)$$

where η is a very small number and Δ_j is the shift in the exciton energy due to its interaction with phonons. This polaronic energy shift can be evaluated using standard techniques based on the polaron model [66]. Without loss in generality, the polaronic shift term can be incorporated as a constituent of the site energy E_l or E_m , and therefore we drop this term from now on. Σ is the self-energy due to dissipative interactions with the phonon bath and other processes associated with exciton recombination, annihilation and trapping which is expressed as

$$\Sigma = \begin{pmatrix} -i(\gamma_{ph,l} + \gamma_{d,l}) & 0 \\ 0 & -i(\gamma_{ph,m} + \gamma_{d,m}) \end{pmatrix}. \quad (10)$$

Here we distinguish the phonon-related dissipative term $\gamma_{ph,j}$ from the dissipative term arising from non-phonon related recombination and trapping effects which is denoted by $\gamma_{d,j}$. $\gamma_{ph,j}$ at site j is obtained as

$$\gamma_{ph,j} = N^{-1} \sum_q |F_j(q)|^2 \delta(\hbar\omega + E_m - E - \Delta p) \quad (11)$$

where E_m is the mean energy of the exciton band, E is the exciton energy and Δp can be interpreted as the dissipative or trap depth [67] which results in the irreversible loss of the exciton. Both E_m and Δp appear as phenomenological constants and their associated values are unavailable for the FMO complex. For the purpose of obtaining numerical values in the next section, we select a range of values for the cumulative term $(\gamma_{ph,j} + \gamma_{d,j})$ and examine its influence on the coherence properties of the excitonic dimer.

Using the inversion procedure adopted by Stafford and Barrett [65], we obtain

$$G(E) = \left(\begin{bmatrix} E - E_l + \frac{i}{2}\bar{\gamma}_l \\ E - E_m + \frac{i}{2}\bar{\gamma}_m \end{bmatrix} - V_r^2 \right)^{-1} \times \begin{bmatrix} E - E_m + \frac{i}{2}\bar{\gamma}_m & V_r \\ V_r & E - E_l + \frac{i}{2}\bar{\gamma}_l \end{bmatrix}. \quad (12)$$

where $\gamma_m = \gamma_{ph,m} + \gamma_{d,m}$ and $\gamma_l = \gamma_{ph,l} + \gamma_{d,l}$. We consider that the exciton in the simple dimer system is initially localized at site $j = l$ at time $t = 0$, thus the probability P_{ll} that the exciton remains at site $j = l$ is determined using $P_{ll}(t) = |G_{11}(t)|^2$. Explicit expressions for $P_{ll}(t)$ and the probability that the exciton has propagated to site $j = m$, $P_{lm}(t)$ can be obtained for equal site energies, $E_l = E_m$ in the coherent tunneling regime ($2V_r > \gamma^*$)

$$P_{ll} = e^{-\bar{\gamma}t} \left[\cos \frac{\Omega}{2}t - \frac{\gamma^*}{\Omega} \sin \frac{\Omega}{2}t \right]^2 \\ P_{lm} = e^{-\bar{\gamma}t} \frac{4V_r^2}{\Omega^2} \sin^2 \frac{\Omega}{2}t, \quad (13)$$

where $\Omega = (4V_r^2 - \gamma^{*2})^{1/2}$, $\gamma^* = \frac{1}{2}(\gamma_m - \gamma_l)$ and $\bar{\gamma} = \frac{1}{2}(\gamma_m + \gamma_l)$. While the contribution of the dissipative term, $\bar{\gamma}$ appears in the exponential function (see Eq.(13)), the dimer can be seen to still exhibit coherence with an effective Rabi oscillation that is influenced by the environment. The system however undergoes incoherent tunneling with loss of Rabi oscillations at $2V_r < \gamma^*$ and we obtain

$$P_{ll} = e^{-\bar{\gamma}t} \left[\cosh \frac{\Omega}{2}t - \frac{\gamma^*}{\Omega} \sinh \frac{\Omega}{2}t \right]^2 \\ P_{lm} = e^{-\bar{\gamma}t} \frac{4V_r^2}{\Omega^2} \sinh^2 \frac{\Omega}{2}t, \quad (14)$$

Due to the presence of a non-Hermitian term in Eqs.(9), (10), the total probabilities, $P_{ll} + P_{lm} \leq 1$ is not conserved and there is loss of normalization which is dependent on the dissipative terms, γ_l and γ_m .

We note that in the case of unequal energies, $E_l \neq E_m$, the dimer system exhibit both incoherent and coherent characteristics with a combination of the terms which appear in Eqs.(13) and (14). In the event of equivalent dissipative couplings at each subsystem, we obtain $\gamma_l = \gamma_m$, $\gamma^* = 0$, and the imaginary term present in Ω vanishes as noted earlier in Ref.[68] for a study involving quantum dot systems. Despite the presence of non-zero γ_l and γ_m , Rabi oscillation of frequency $\Omega = \sqrt{4V_r^2 + (E_l - E_m)^2}$ occurs. The subsystems of the dimer can be considered to be unmeasured by the environmental sources when there is equivalent couplings to the dissipation channels, an observation that was first noted by Stafford and Barrett [65] for super deformed nuclei systems. In this regard the indistinguishability of the source of decoherence preserves the coherence of the excitonic dimer in photosynthetic systems.

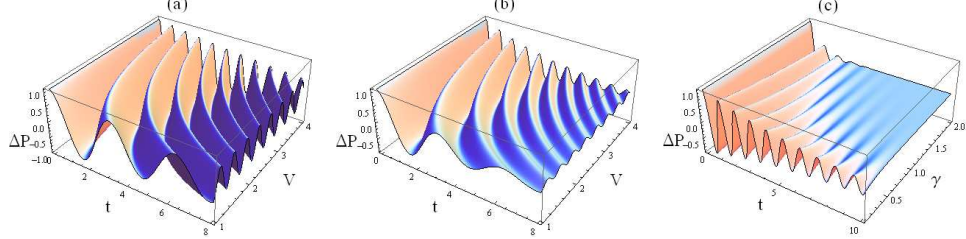


FIG. 1: (a) The exciton population difference, $\Delta P = P_l - P_{lm}$ as a function of time t , and the bare intersite coupling energy, V at dissipation rates $\gamma_m = \gamma_l = 0.1$ for the degenerate case ($E_l = E_m$). The units are chosen such that $\hbar = 1$, and the phonon bath response time, $\omega_0 = 1$.

(b) $\Delta P = P_l - P_{lm}$ as a function of time t , the bare intersite coupling energy, V at dissipation rates $\gamma_m = 0.1$, $\gamma_l = 0.5$.

(c) $\Delta P = P_l - P_{lm}$ as function of time t and dissipation rate γ_m , at $\gamma_l = 0.2$ and $V = 3$.

In order to examine the effect of the intersite coupling energy, V and the dissipation rates γ_m , γ_l on the exciton dynamics, we consider the bare intersite energy V without the Franck-Cordon (FC) factor [64]. Figure 1a,b,c shows the coherence properties as reflected in the exciton population difference, $\Delta P = P_l - P_{lm}$ as a function of time and the bare intersite coupling energy, V . We note that an increase in the strength of intersite energy V increases the time period over which the population difference, ΔP which is a signature of coherence, is maintained. As illustrated in Figure 1c, the gradual increase in one of the dissipation rate γ_m erodes the coherence in the dimer system as time progresses.

III. PHOTOSYNTHETIC QUBITS AND APPEARANCE OF EXCEPTIONAL POINTS

Following Eq.(12) and the form of the occupation probabilities in Eqs.(13) and (14), the symmetric and anti-symmetric states of the dimer system at the resonance point ($E_l = E_m$) is obtained as

$$\begin{aligned}
 |\chi_s(t)\rangle &= e^{-\bar{\gamma}t/2} \left(\cos \frac{\Omega}{2}t - i \cos \theta \sin \frac{\Omega}{2}t \right) |\mathbf{l}\rangle \\
 &\quad + i e^{-\bar{\gamma}t/2} \sin \theta \sin \frac{\Omega}{2}t |\mathbf{m}\rangle \\
 |\chi_a(t)\rangle &= e^{-\bar{\gamma}t/2} \left(\cos \frac{\Omega}{2}t - i \cos \theta \sin \frac{\Omega}{2}t \right) |\mathbf{l}\rangle \\
 &\quad - i e^{-\bar{\gamma}t/2} \sin \theta \sin \frac{\Omega}{2}t |\mathbf{m}\rangle,
 \end{aligned} \tag{15}$$

where $\cos \theta = \frac{i\gamma^*}{\Omega}$ and Ω and γ^* are defined below Eqs.(13). The excitonic qubits states in Eqs.(15) are coded using the relative position of the exciton via the basis set, ($|\mathbf{l}\rangle, |\mathbf{m}\rangle$)

$$\begin{aligned}
 |\mathbf{l}\rangle &= |\Xi_l\rangle \otimes |\mathbf{0}\rangle_m \\
 |\mathbf{m}\rangle &= |\mathbf{0}\rangle_l \otimes |\Xi_m\rangle,
 \end{aligned} \tag{16}$$

where $|\Xi_l\rangle$ ($|\Xi_m\rangle$) denote the excitonic state at site l (m), and the state $|\mathbf{0}\rangle_l$ ($|\mathbf{0}\rangle_m$) denote the ground states at site l (m) (the absence of exciton). Other than the qubit states, $|\chi_s(t)\rangle$ and $|\chi_a(t)\rangle$, entangled states of the form $|\mathbf{0}\rangle_l |\mathbf{0}\rangle_m$ and $|\Xi_l\rangle |\Xi_m\rangle$ may also result in the dimer system.

At unequal energies, $E_l \neq E_m$, the states equivalent to the symmetric and asymmetric states in Eq.(15) possess eigenenergies of the form

$$E_{\pm} = \bar{E}_l + \bar{E}_m \pm \sqrt{(\bar{E}_m - \bar{E}_l)^2 + 4V_r^2}. \quad (17)$$

where the complex energy levels $\bar{E}_l = E_l - i\gamma_l$ and $\bar{E}_m = E_m - i\gamma_m$ and the dissipative terms γ_m and γ_l are specified below Eq.(13). The excitonic qubit oscillates coherently between the two dots with the complex Rabi frequency $E_+ - E_- = \bar{\omega} = 2 \sqrt{[(\bar{E}_m - \bar{E}_l)^2 + 4V_r^2]}^{1/2}$. By setting $E_l = E_m$, the eigenenergies corresponding to Eq.(15) can be easily evaluated. The real component of $\bar{\omega}$ correspond to Rabi oscillations while the imaginary component correspond to the rate of incoherent tunneling [68]. The role of a complex Rabi frequency has been discussed [68] in the context of the double quantum dot system coupled to a continuum of states.

Due to the presence of non-Hermitian terms, we write the adjoint symmetric and anti-symmetric states corresponding to the states in Eq.(15) as

$$\begin{aligned} |\tilde{\chi}_s(t)\rangle &= e^{-\bar{\gamma}t/2} \left(\cos \frac{\Omega}{2}t + i \cos \theta \sin \frac{\Omega}{2}t \right) |l\rangle \\ &\quad - i e^{-\bar{\gamma}t/2} \sin \theta \sin \frac{\Omega}{2}t |m\rangle \\ |\tilde{\chi}_a(t)\rangle &= e^{-\bar{\gamma}t/2} \left(\cos \frac{\Omega}{2}t + i \cos \theta \sin \frac{\Omega}{2}t \right) |l\rangle \\ &\quad + i e^{-\bar{\gamma}t/2} \sin \theta \sin \frac{\Omega}{2}t |m\rangle, \end{aligned} \quad (18)$$

In the case of strong dissipative processes and at rising temperatures, it is likely that the condition $2V_r = \gamma^*$ will be satisfied and $\Omega=0$. This signifies the appearance of the exceptional point [55] when both coherent and incoherent tunneling regimes merge, and the two eigenvalues coalesce to represent just one eigenfunction. We obtain $P_{ll} = \left(1 - \frac{\gamma^*t}{2}\right)^2 e^{-\bar{\gamma}t}$, $P_{lm} = \left(\frac{\gamma^*t}{2}\right)^2 e^{-\bar{\gamma}t}$ and the population difference $P_{ll} - P_{lm} = (1 - \gamma^*t) e^{-\bar{\gamma}t}$

IV. APPLICATION TO THE B850 BCHLS DIMER MODEL

The LH2 B850 pigment-protein complex which interacts with the reaction center via LH1, consists of a cyclic array of polypeptide heterodimers, with each polypeptide pair of $\alpha\beta$ subunit, containing three Bchls. A pair of Bchls is located near the outer membrane surface of the complex, while a single Bchl is present near the inner membrane as detailed in Ref.[48]. A similar cyclic structure (B800 ring), but one with a smaller number of Bchls accounts for the 800 nm absorption spectrum of the LH2 complex. We utilize a simple model which consists of two coupled B850 Bchls, each BChl with a two-state structure forming the basis of the Q_y one-exciton states. The Q_y bandwidth is associated with the lowest excited state of the BChl molecule. The two-state model of the BChl interacts with its surrounding phonon bath with properties similar to that of a spin-boson system [64], and forms an integral part of light-harvesting energy transfer mechanisms in the LH2 B850 pigment-protein complex.

We employ the Hamiltonian of the form given in Eq. (3) to represent the B850 Bchls dimer, with the intersite coupling energy $V=250 \text{ cm}^{-1}$ and consider the two site energies to be equal, that is $E_l \approx E_m$. We use the spectral density function associated with the overdamped Brownian oscillator [69]

$$J(\omega) = \frac{2}{\pi} \lambda_b \omega_0 \frac{\omega}{\omega^2 + \omega_0^2} \quad (19)$$

where λ_b is the bath reorganization energy and ω_0 is a frequency cutoff for the bath. We use values of $\lambda_b = 200 \text{ cm}^{-1}$ and $\hbar\omega_0 = 50 \text{ cm}^{-1}$ which are acceptable estimates in photosynthetic systems [6, 12, 18, 19, 48]. It is expected that the bath reorganization energy λ_b has an implicit dependence on temperature, however here we assume that it remains independent of temperature for the sake of obtaining some numerical estimates of the dynamics of energy exchange in the B850 Bchls system.

The effect of temperature on the time evolution of the population difference, $\Delta P = P_{ll} - P_{lm}$, at various dissipation levels is shown in Fig. 2a,b,c. While oscillations are preserved at small dissipation levels up to moderate temperatures (80 K), there is less exchange of energy between the two sites at the comparatively larger temperatures (140 K). Moreover the probabilities of site occupation P_{ll} and P_{lm} becomes zero due to outflow of energy to the dissipation

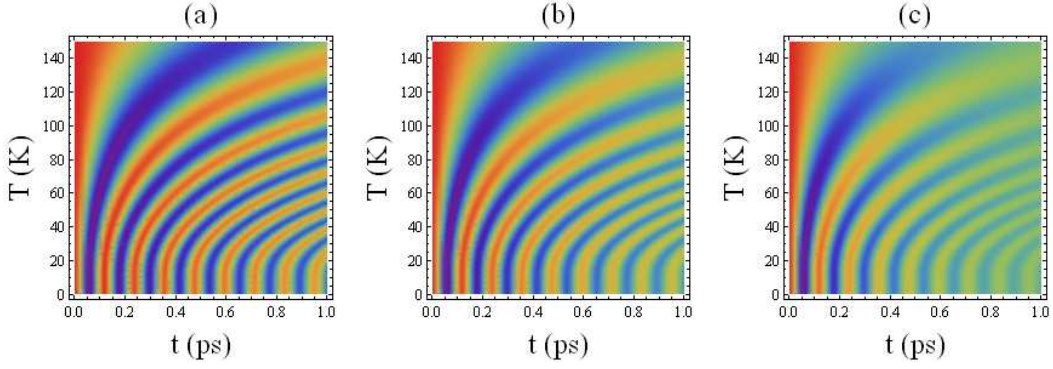


FIG. 2: Fading out of the exciton population difference, $\Delta P = P_l - P_{lm}$, with increase in time (ps) and temperature (in K) at various dissipation strengths, $\gamma_m = \gamma_l =$ (a) 2.5 cm^{-1} (b) 5 cm^{-1} (c) 10 cm^{-1} . The bath reorganization energy $\lambda_b = 200 \text{ cm}^{-1}$, $\hbar\omega_0 = 50 \text{ cm}^{-1}$ and bare intersite coupling energy, $V = 250 \text{ cm}^{-1}$ [6, 12, 18, 48]. The colour shading range from red for the maximum population difference of 1 to blue for the minimum population difference of -1.

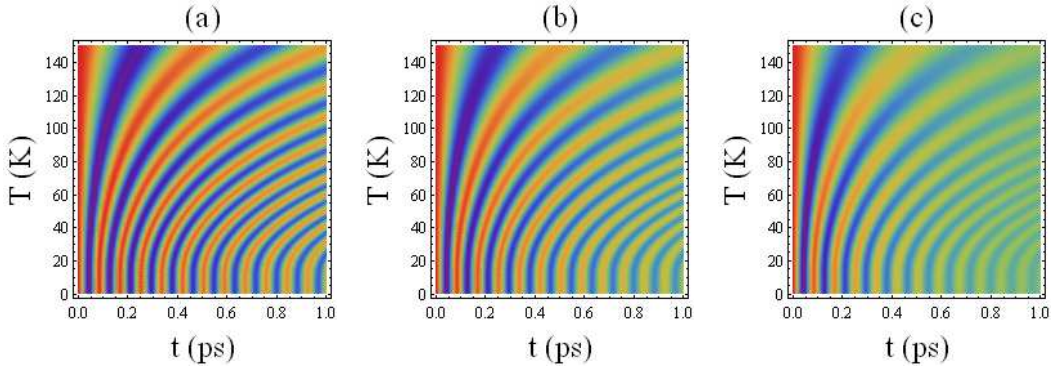


FIG. 3: Population difference, $\Delta P = P_l - P_{lm}$ as function of time (ps) and temperature (in K) at various dissipation strengths, $\gamma_m = \gamma_l =$ (a) 2.5 cm^{-1} (b) 5 cm^{-1} (c) 10 cm^{-1} . The bath reorganization energy is set lower at $\lambda_b = 150 \text{ cm}^{-1}$. All other parameters ($\hbar\omega_0, V$) and colour codes are set at the same values as specified in the caption of Fig. 2.

sources. We note increased oscillations in ΔP as illustrated in Fig. 3a,b,c when the bath reorganization energy is reduced to a lower value of $\lambda_b = 150 \text{ cm}^{-1}$. As mentioned earlier, the results in these figures are based on the assumption that the reorganization energy is independent of the temperature, which has been used in earlier works [19, 48]. Currently, the explicit dependence of λ_b on the temperature is lacking in the literature. The effect of including the temperature dependence of λ_b is expected to alter the quantitative estimates of the timescale of oscillations by a small factor, however we expect the salient qualitative features to be preserved. It is to be noted that the time estimates obtained using our simple dimer model is in partial agreement with experimental results [29, 31] which show that coherent oscillations persist up to 0.3 ps even at physiological temperatures for a similar photosynthetic system. The oscillations in population difference ΔP as illustrated in Figs. 2, 3 are clearly dependent on the strength of exciton coupling to the sources of dissipation and the estimates in the range (2 to 10) cm^{-1} employed here may be lower than those in photosynthetic systems. Accordingly, recombination and trapping effects which are common sources of dissipation, are expected to have a significant effect on the photosynthetic activity of light harvesting systems in general.

Fig. 4 illustrates the dependence of the critical temperatures (K) which occur at exceptional points, as a function of the dissipation strength difference, $\Delta\gamma = |\gamma_m - \gamma_l|$ based on Eq.(17). The results indicate that some degree of coherence can be obtained at physiologically higher temperatures ($> 70\text{K}$) as long as the dissipation strength difference, $\Delta\gamma$ is kept low. It is to be noted that the estimates of the critical temperatures in Fig. 4 is based on a simple dimer model which circumvents comprehensive details that incorporate the energy bias and solvent relaxation rate, various kinetic behaviors of the electron transfer mechanisms and dynamic bath effects as considered in Ref.[70]. In general, the Redfield model employed here works well as a weak coupling model, however its validity is very much dependent on the partitioning between the exciton Hamiltonian and the intersite coupling and exciton-phonon terms. In Eq. (3) we have chosen the exciton states as the zeroth order term, which may not provide a reliable description of

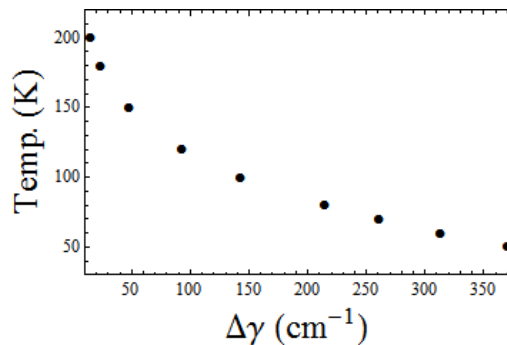


FIG. 4: Critical temperatures (K) at which exceptional points occur, as a function of the dissipation strength difference, $\Delta\gamma=|\gamma_m-\gamma_l|$. All other parameters ($\hbar\omega_0$, λ_b , V) are set at the same values as specified in the caption of Fig. 2.

the dynamics in light-harvesting complexes, under certain environmental conditions [46]. It has been noted earlier that the secular Redfield equation [45] leads to an overestimation of the environment-assisted transfer process which results in inaccuracies in the prediction of the coherent-incoherent transition region. One approach of overcoming this problem is by extending Eq. (3) to dressed excitons or composite exciton-phonon states with hybrid exciton-phonon characteristics. This can be done using suitable canonical transformations of exciton and phonon operators to a transformed Hilbert space, however analytical solutions can only be obtained under strict limits. While the analytical model employed here offers advantage in the computational speed of prediction of the exception point, we expect some quantitative changes (less than an order of magnitude) in the critical temperatures shown in Fig. 4 when improved models incorporating more realistic features are utilized. Nevertheless, the qualitative trends, especially changes in the exceptional point temperatures with dissipation strength differences, are expected to be unaffected by the assumptions inherent in the Redfield model for the range of $\Delta\gamma$ and bath reorganization energies considered in this work. In this regard, the underlying principles associated with the appearances of exceptional points can be generalized to studies which include more elaborate system parameters. Hence there is ample scope to extend the intermediate complexity of the current work to scrutinize the factors which influence the crossover point from coherent to incoherent dynamics, and influence the appearance of exceptional points in more realistic systems with strong system-bath couplings.

The connection between the exactly solvable two-state model to light-harvesting energy transfer processes should also be viewed in the context of the large molecular structure of realistic photosynthetic systems. Extrinsic factors such as network size and topological connectivity present in large molecular structures assume vital roles in the optimum energy transfer processes, and consequently determine the coherence properties of the entangled exciton in large molecular structures. In a recent work [71], the mapping of quantum energy transfer processes to network kinetics with nonlocal connectivity was examined in three-level systems, linear-chains, and other closed networks. The results indicated that environments can be optimized to maximize energy transfer efficiency, with prediction of phase-sensitive interferences in closed-loop configurations. These factors provide sufficient framework to examine the appearances of exceptional points within the structure of large topologically connected structures and their possible influence on phase-sensitive interferences [71].

V. THE QUANTUM BRACHISTOCHRONE PASSAGE TIMES IN PHOTOSYNTHETIC SYSTEMS.

The exact role of exceptional points in photosynthetic systems remains unclear, and it is likely that these points are linked to the quantum non-Hermitian brachistochrone problem [72, 73]. In the general brachistochrone problem, the minimum time taken to transverse the path between two locations of a particle is determined, this becomes the quantum brachistochrone problem when the time of evolution of the quantum system between two states is required. It has been shown that the passage time of evolution of an initial state into the final state can be made arbitrarily small for a time-evolution operator that is non-Hermitian but PT -symmetric [73]. This result has recently been generalized to non- PT -symmetric dissipative systems [74]. The results in Refs. [73, 74] appear to suggest that the timescales of propagation in non-Hermitian quantum mechanics are faster than those of Hermitian systems. Using the approach detailed in Ref. [74], we compute the passage time, τ_p taken for the $|l\rangle$ state to make a transition to the $|m\rangle$ state as a function of temperature and the dissipation strength difference, $\Delta\gamma=|\gamma_m-\gamma_l|$ (Fig. 5).

As expected, τ_p increases with temperature, however it decreases with the dissipation strength difference, $\Delta\gamma$. The passage times (in ps) obtained here are small compared to typical estimates (1 ns) of the fluorescence decay times of

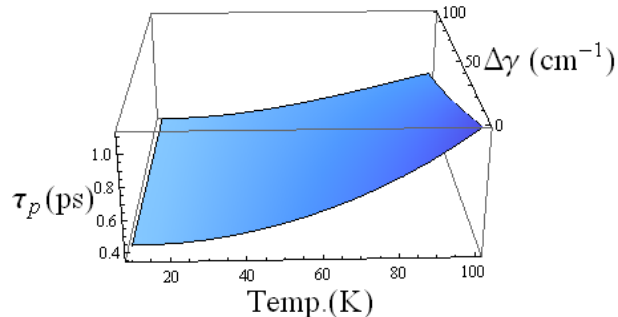


FIG. 5: Passage time from the $|l\rangle$ to $|m\rangle$ states as a function of the dissipation strength difference, $\Delta\gamma=|\gamma_m-\gamma_l|$ and temperature. The bath reorganization energy $\lambda_b=150\text{ cm}^{-1}$, $\hbar\omega_0 = 50\text{ cm}^{-1}$ and bare intersite coupling energy, $V=250\text{ cm}^{-1}$

the light harvesting complex [15]. This suggest considerable delocalization, with implications for non-trivial quantum correlations amongst various pigment sites. However the explicit link between the entanglement properties and the brachistochrone passage times is not well understood. There is some consistency of the results in Fig. 5 with earlier results which show loss of coherence at physiologically higher temperatures (Fig. 4), however the decrease of τ_p with the dissipation strength difference, $\Delta\gamma=|\gamma_m-\gamma_l|$ may be associated with a decrease in efficiency of the energy transfer mechanism. Clearly there are open questions with regard to the entanglement properties of quantum systems which obey non-Hermitian quantum dynamics, these properties are comparatively well established in Hermitian systems. For instance there is lack of consensus on the properties of the non-Hermitian eigenstates, as while it is known that real eigenstates are associated with localized states, eigenvalues of non-Hermitian eigenstates may have complex delocalization features which are not well understood [75].

The results obtained here can be compared to earlier works [76–78] of coherent exciton dynamics which show that the environment not only allow the preservation of some coherent features but also assist in the quantum transport in light-harvesting systems, even at ambient temperatures. However the role of exceptional points have not been implicated in the earlier works, and in this respect, the estimates of the quantum brachistochrone passage times here is expected to bring greater depth to existing studies in this field. Hence the solvable model examined in this work suggest features that have not been predicted in earlier works. Nevertheless, the role of new measures of quantum correlations which possess more generalized properties such as the quantum discord [79, 80] in the photosynthetic process needs further investigation, including examination of the intricate links between the exceptional point and quantum correlation measures.

Lastly, we have presented calculations associated with a dissipative two-level dimer model which incorporates decay terms due to coupling to a macroscopic environment. The results when applied to the B850 Bchls dimer system can account partly for the observed high efficiencies of energy transfer in light harvesting systems, and highlight the critical link between photosynthetic coherences and dissipation strength differences at the two sites of the dimer. There is greater efficiency in energy transfer as long as the distinguishability of the subunits of the dimer is minimized, an analogous observation was made for the system of quantum dot systems connected to conducting leads in an earlier work[68]. Thus in the presence of a small dissipation strength difference, $\Delta\gamma$ the excitonic coherences appear insensitive to the environmental changes, provided the subunits are not distinguished by varying the strength of dissipation. The most important result of this study is however related to the appearance of the exceptional point which has not received attention in earlier works on photosynthetic systems. Despite the frequent mention of the crossover point from coherent to incoherent dynamics at increasing temperatures in the literature, the presence of the exceptional points has been overlooked. The evaluation of the quantum brachistochrone passage times is also unique to this work. However the role of exceptional points need further investigations, as there are many unanswered questions as to how such points actually related to the high efficiencies measure in light harvesting systems.

It is to be noted that the model used in this work can be applied to obtain numerical estimates of quantum coherence in other photosynthetic systems which possess more realistic spectral functions associated with the environmental couplings. The model used here can also be extended to examine the properties of the exceptional points and the quantum brachistochrone passage times in a dimer model where the onsite and coupling energies differ as well. It is expected that the qualitative features involving the appearances of exceptional points, and shown within the intermediate complexity of the current work, are expected to be retained in more sophisticated models. In this regard,

the results obtained in the current work provide important guidelines for future investigations in more sophisticated models, and in the detection and control of quantum effects in artificial photosynthetic systems.

VI. ACKNOWLEDGMENTS

This research was undertaken on the NCI National Facility in Canberra, Australia, which is supported by the Australian Commonwealth Government.

-
- [1] J. J. Hopfield, Proc. Nat. Acad. Sci. U.S.A., **71**, 3640 (1974).
 [2] Th. Frster, Ann. Phys. **437**, 55 (1948).
 [3] H. Zuber and R. Cogdell, in *Anoxygenic Photosynthetic Bacteria*, edited by R. Blankenship, M. Madigan, and C. Bauer, pp. 315348 (Kluwer Academic, Dordrecht, 1995).
 [4] B. Chance and M. Nishimura, Proc. Nat. Acad. Sci. U.S.A., **46**, 19 (1960).
 [5] R. S. Knox, in *Primary Processes of Photosynthesis*, edited by J. Barber, pp. 5597 (Elsevier, Amsterdam, 1977).
 [6] *Light-Harvesting Antennas in Photosynthesis*, edited by B. R. Green and W. W. Parson (Springer, New York, 2003).
 [7] V. May and O. Kühn, *Charge and Energy Transfer Dynamics in Molecular Systems*, 2nd ed. (Wiley-VCH, Berlin, 2004).
 [8] B. Happ, J. Schäfer, R. Menzel, M. D Hager, A. Winter, J. Popp, R. Beckert, B. Dietzek and U. S. Schubert, *Macromolecules*, **44**, 6277, (2011).
 [9] M. Mohseni, P. Rebentrost, S. Lloyd and A. Aspuru-Guzik, *J. Chem. Phys.* **129**, 174106 (2008).
 [10] E. N. Zimanyi and R. J. Silbey, *J. Chem. Phys.* **133**, 144107 (2010).
 [11] P. K. Ghosh, A. Y. Smirnov and F. Nori, *J. Chem. Phys.* **134**, 244103 (2011).
 [12] C. Olbrich, T. L. C. Jansen, J. Liebers, M. Aghtar, J. Strümpfer, K. Schulten, J. Knoester, and U. Kleinekathöfer, *J. Phys. Chem. B*, **115**, 8609 (2011).
 [13] H. van Amerongen and R. van Grondelle, *J. Phys. Chem. B* **105**, 604 (2001).
 [14] P. Horton, and A. V. Ruban, *J. Exp. Bot.* **56**, 365 (2005).
 [15] M. A. Palacios, F. L. de Weerd, J. A. Ihalainen, R. van Grondelle, and H. van Amerongen, *J. Phys. Chem. B* **106**, 5782 (2002).
 [16] T. Brixner, J. Stenger, H. M. Vaswani, M. Cho, R. E. Blankenship, and G. R. Fleming, *Nature*, **434**, 625 (2005).
 [17] R. E. Fenna and B. W. Matthews, *Nature*, **258**, 573 (1975).
 [18] G. S. Engel, T. R. Calhoun, E. L. Read, T.K. Ahn, T. Mancal, Y. C. Cheng, R. E. Blankenship, and G. R. Fleming, *Nature*, **446**, 782 (2007).
 [19] N. Renaud, M. A. Ratner and V. Mujica, *J. Chem. Phys.* **135**, 075102 (2011).
 [20] J. Adolphs and T. Renger, *Biophys. J.* **91**, 2778 (2006).
 [21] B. Bruggemann, P. Kjellberg, and T. Pullerits, *Chem. Phys. Lett.* **444**, 192 (2007).
 [22] R. Siebert, A. Winter, B. Dietzek, U. Schubert, J. Popp, *J. Macromol. Rapid Commun.*, **31**, 883 (2010).
 [23] J. Schaefer, R. Menzel, D. Weiss, B. Dietzek, R. Beckert, J. Popp, *Journal of Luminescence*, **131**, 1149 (2011).
 [24] H. Dürr and S. Bossmann, *Acc. Chem. Res.*, **34**, 905 (2001).
 [25] W. D. Larkum, *Curr. Opin. Biotechnol.* **21**, 271 (2010).
 [26] Y. Terazono, G. Kodis, P. A. Liddell, V. Garg, T. A. Moore, A. L. Moore, and D. Gust, *J. Phys. Chem. B*, **113**, 7147 (2009).
 [27] R. M. Clegg, M. Sener and Govindjee, *Proc. SPIE* **7561**, 75610C (2010).
 [28] D. Gust, T. A. Moore, and A. L. Moore, *Acc. Chem. Res.*, **34**, 40 (2001).
 [29] E. Collini, C. Y. Wong, K. E. Wilk, P. M.G. Curmi, P. Brumer, and G. D. Scholes, *Nature*, **463**, 644 (2010).
 [30] M. Cho, H. M. Vaswani, T. Brixner, J. Stenger, and G. R. Fleming, *J. Phys. Chem. B* **109**, 10542 (2005).
 [31] G. Panitchayangkoon, D. Hayes, K. A. Fransted, J. R. Caram, E. Harel, J. Wen, R. Blankenship, G. S. Engel, *Proc. Nat. Acad. Sci.* **107**, 12766 (2010).
 [32] D. Segale and V. A. Apkarian, *J. Chem. Phys.* **135**, 024203 (2011).
 [33] F. Galve, L. A. Pachon and D. Zueco, *Phys. Rev. Lett.* **105**, 180501 (2010).
 [34] F. Fassioli and A. Olaya-Castro, *New J. Phys.* **12**, 085006 (2010).
 [35] F. Caruso, A. W. Chin, A. Datta, S. F. Huelga and M. B. Plenio, *Phys. Rev. A* **81**, 062346 (2010).
 [36] M. Sarovar, A. Ishizaki, G. R. Fleming and K. B. Whaley, *Nature Physics* **6**, 462 (2010).
 [37] T. Scholak, F. de Melo, T. Wellens, F. Mintert, A. Buchleitner, *Phys. Rev. E* **83**, 021912 (2011).
 [38] A. Nazir, *Phys. Rev. Lett.* **103**, 146404 (2009).
 [39] F. Fassioli, A. Nazir, A. J. Olaya-Castro, *Phys. Chem. Lett.* **1**, 2139 (2010).
 [40] P. Nalbach, J. Eckel, M. Thorwart, *New J. Phys.* **12**, 065043 (2010).
 [41] A.G. Redfield, *Advances in Magnetic Resonance* (Academic Press Inc., New York, 1965), **1**, pp. 132.
 [42] U. Weiss, *Quantum Dissipative Systems*, (World Scientific, Singapore, 1993).
 [43] H. P. Breuer and F. Petruccione, *The Theory of Open Quantum Systems* (Oxford University Press, New York, 2002).
 [44] E. O. Potma and D. A. Wiersma, *J. Chem. Phys.*, **108**, 4894 (1998).

- [45] A. Ishizaki and G. R. Fleming, *J. Chem. Phys.* **130**, 234111 (2009).
- [46] J. Wu, F. Liu, Y. Shen, J. Cao and R. J. Silbey, *New J. Phys.* **12**, 105012 (2010).
- [47] D. Abramavicius and S. Mukamel, *J. Chem. Phys.* **133**, 064510 (2010).
- [48] J. Strümpfer and K. Schulten, *J. Chem. Phys.* **134**, 095102 (2011).
- [49] E. N. Economou, *Greens Functions in Quantum Physics* (Springer-Verlag, Berlin, 1979).
- [50] J. Malinsky and Y. Magarshak, *J. Phys. Chem.*, **96**, 2849 (1992).
- [51] A. Suna, *Phys. Rev.* **135**, A111 (1964).
- [52] A. S. Davydov, *Theory of Molecular Excitons* (Plenum, New York, 1971).
- [53] A. Thilagam, *J. Phys. A: Math. Theor.* **43** 155301 (2011).
- [54] E. Teller, *J. Phys. Chem.* **41**, 109 (1937).
- [55] W. D. Heiss and A. L. Sannino, *Phys. Rev. A* **43**, 4159 (1991).
- [56] A. Thilagam, *J. Phys. A: Math. Theor.* **43** 354004 (2010).
- [57] C. Dembowski, B. Dietz, H. D. Gräf, H. L. Harney, A. Heine, W. D. Heiss and A. Richter 2001 *Phys. Rev. Lett.* **90**, 034101 (2003).
- [58] B. Dietz, T. Friedrich, J. Metz, M. Miski-Oglu, A. Richter, F. Schäfer, and C. A. Stafford, *Phys. Rev. E* **75**, 027201 (2007).
- [59] C. Dembowski, B. Dietz, H. D. Gräf, H. L. Harney, A. Heine, W. D. Heiss, and A. Richter, *Phys. Rev. E* **69**, 056216 (2004).
- [60] G. Khitrova, H. M. Gibbs, M. Kira, S. W. Koch, and A. Scherer, *Nat. Phys.* **2**, 81 (2006).
- [61] R. Lefebvre, O. Atabek, M. Sindelka, and N. Moiseyev, *Phys. Rev. Lett.* **103**, 123003 (2009).
- [62] R. Uzdin and R. Lefebvre, *J. Phys. B: At. Mol. Opt. Phys.* **43**, 235004 (2010).
- [63] H. Cartarius, J. Main, and G. Wunner, *Phys. Rev. Lett.* **99**, 173003 (2007).
- [64] A. J. Leggett, S. Chakravarty, A. T. Dorsey, M. P. A. Fisher, A. Garg, and W. Zwerger, *Rev. Mod. Phys.* **59**, 1 (1987).
- [65] C. A. Stafford and B. R. Barrett, *Phys. Rev. C* **60** 051305, (1999).
- [66] G. D. Mahan, *Many Particle Physics*, (Plenum, New York, 2000).
- [67] A. Thilagam, *Phys. Rev. A* **81**, 032309 (2010).
- [68] D. M. Cardamone, C. A. Stafford, and B. R. Barrett, *Phys. stat. sol. (b)*, **230**, 419 (2002).
- [69] S. Mukamel, *Principles of Nonlinear Optics and Spectroscopy* (Oxford University Press, New York, 1995).
- [70] Y. J. Jung and J. Cao, *J. Chem. Phys.* **117**, 3822 (2007).
- [71] J. Cao and R. J. Silbey, *J. Phys. Chem. A*, **113**, 13825 (2009).
- [72] A. Mostafazadeh, *Phys. Rev. Lett.* **99** 130502 (2007).
- [73] C. M. Bender, D. C. Brody, H. F. Jones and B. K. Meister, *Phys. Rev. Lett.* **98**, 040403 (2007).
- [74] P. E. Assis and A. Fring, *J. Phys. A: Math. Theor.* **41**, 244002 (2008).
- [75] N. Hatano and D. R. Nelson, *Phys. Rev. B* **58**, 8384 (1998).
- [76] F. Caruso, A. W. Chin, A. Datta, S. F. Huelga and M. B. Plenio, *J. Chem. Phys.* **131**, 105106 (2009).
- [77] P. Rebentrost, M. Mohseni, I. Kassal, S. Lloyd and A. Aspuru-Guzik, *New. J. Phys.* **11**, 033003 (2009).
- [78] O. Müllen and T. Schmid, *Phys. Rev. E* **82**, 042104 (2010).
- [79] H. Ollivier and W. H. Zurek, *Phys. Rev. Lett.* **88**, 017901 (2001).
- [80] L. Henderson and V. Vedral, *J. Phys. A* **34**, 6899 (2001).